CHEMISTRY
A EUROPEAN JOURNAL

DOI: 10.1002/chem.200701591

Visualizing the Crystal Structure and Locating the Catalytic Activity of Micro- and Mesoporous ZSM-5 Zeolite Crystals by Using In Situ Optical and Fluorescence Microscopy

Marianne H. F. Kox,[a] Eli Stavitski,[a] Johan C. Groen,[b] Javier Pérez-Ramírez,[c] Freek Kapteijn,[b] and Bert M. Weckhuysen*[a]

Abstract: A combination of optical and fluorescence microscopy was used to study the morphology of micro- and mesoporous H-ZSM-5 zeolite crystals ($17\times4\times4$ μm) and to evaluate, in a spatially resolved manner, the effect of mesoporosity, introduced via desilication, on catalytic performance. For this purpose, the oligomerization of various styrene molecules was used as a model reaction, in which the carbocation intermediates formed in the zeolite pores act as reporter molecules. In situ confocal fluorescence measurements after the template removal process showed that the crystals generally consist of three different subunits that have pyramidal boundaries with each other. Examination of these crystals during styrene oligomerization revealed differences in the catalytic activity between the purely microporous and the combined micro- and mesoporous crystals. The introduction of intracrystalline mesoporosity limits the formation to dimeric carbocation intermediates and facilitates the transport of styrene molecules inside the zeolite volume. This leads to a more uniform coloration and fluorescence pattern of the crystals. Moreover, the oligomerization of various styrene compounds, which differ in their reactivity, provides a good way of estimating the Brønsted acid strength in a spatially resolved manner, showing a non-homogeneously distributed Brønsted acidity over the volume of the crystals. More detailed information on the structure of the ZSM-5 crystals was revealed for mesoporous crystals during the oligomerization of 4-methoxystyrene. This reaction induced an "explosion" of the crystal leading to the formation of a complex system with at least eight different subunits. Finally, polarized-light microscopy was used to unravel the pore geometry in these individual building blocks. The observed differences in catalytic behavior between micro- and mesoporous ZSM-5 crystals are strengthened by the microspectroscopic techniques employed, which show that upon desilication the crystal morphology is affected, the product distribution is changed towards less conjugated carbocation intermediates, and that a gradient in Brønsted acid strength appears to be present.

Keywords: fluorescence · mesoporous materials · microspectroscopy · oligomerization · zeolites

Introduction

Zeolites are an important class of microporous crystalline aluminosilicates. Due to the unique combination of acid properties and a well-defined framework, zeolites with the MFI topology are widely used as catalysts in many industrial applications, such as oil refining, petrochemistry, and the manufacture of organic intermediates in the fine chemical industry.[1] However, the purely microporous character of zeolites often results in a reduced catalytic activity due to diffusion limitations. To alleviate this, several approaches are practiced to enhance mass transport in the pores of the zeolite, for example, synthesis of zeolite particles in the nanometer range (<200 nm),[2] synthesis of wide-pore zeolite crystals,[3,4] and delamination of lamellar zeolite precur-

[a] M. H. F. Kox, Dr. E. Stavitski, Prof. Dr. B. M. Weckhuysen
Inorganic Chemistry and Catalysis Group
Department of Chemistry
Utrecht University
Sorbonnelaan 16, 3584 CA Utrecht (The Netherlands)
Fax: (+31) 30-251-1027
E-mail: b.m.weckhuysen@chem.uu.nl

[b] Dr. J. C. Groen, Prof. Dr. F. Kapteijn
Catalysis Engineering, DelftChemTech
Delft University of Technology
Julianalaan 136, 2628 BL Delft (The Netherlands)

[c] Prof. Dr. J. Pérez-Ramírez
ICREA and Institute of Chemical Research of Catalonia (ICIQ)
Av. Països Catalans 16, 43007 Tarragona (Spain)

sors.[5] Another way to increase diffusion properties without affecting the channel framework is the synthesis of hierarchical zeolitic materials with introduced mesoporosity. Commonly used methods include the preparation of composite materials in which zeolite domains are embedded in mesoporous supports, the synthesis of micro- and mesoporous zeolitic material through carbon templating, soft templating using multifunctional surfactants, and dealumination by hydrothermal treatment or acid leaching.[6–11] The latter method, in which aluminum is selectively removed from the zeolite framework, has been successfully applied to create mesoporosity in zeolite Y and mordenite. One of the main drawbacks of this method is that the Brønsted acidity of the zeolite material is severely affected, and the materials may thus become less suitable for acid-catalyzed reactions. Moreover, it has been demonstrated that this postsynthesis modification treatment most often leads to encapsulated porosity,[12,13] which is not readily accessible and, therefore, only contributes to the improved diffusion in a limited way.

Recently, Groen et al. developed a novel postsynthesis treatment to introduce mesoporosity into the zeolite framework.[14–20] In contrast to dealumination, silicon is selectively extracted from the framework in alkaline media, thereby creating mesopores without, in principle, affecting the Brønsted acidity. This approach has been successfully applied to both ZSM-5[21] and mordenite crystals.[22] Transient uptake measurements of neopentane over large crystals demonstrated a two orders of magnitude higher rate of diffusion for the combined micro- and mesoporous zeolite as compared to the purely microporous parent sample. Apart from this key result, little is known about the role of the mesopores during catalytic reactions, that is, whether their surface participates in the catalytic reaction or merely provides highways to the Brønsted acid sites confined in the micropores; also, the exact location in the crystal is not precisely known. In 2002, Corma et al. suggested, based on measurements with di-*tert*-butylpyridine, that the external surface (mesopore walls) exhibits acidic properties and thus could participate in acid-catalyzed conversions.[23]

Herein, we study the microporous and combined micro- and mesoporous (subsequently referred to as desilicated or mesoporous) ZSM-5 crystals synthesized by Groen et al.,[24] making use of in situ microspectroscopic techniques. To examine the intergrowth structure of these zeolite materials, confocal fluorescence microscopy was employed, based on the mapping of the template removal process in individual crystals.[25] The effect of mesoporosity on the shape selectivity and catalytic activity was studied by the oligomerization of different styrene compounds.[26,27] Furthermore, optical microspectroscopic examination by using polarized light revealed the microscopic alignment of styrene product molecules in the micropores of the zeolite crystals and, hence, the pore orientation.

Results and Discussion

Detailed information on the combined approach developed in our laboratory, based on confocal fluorescence microscopy and polarized-light optical microspectroscopy, can be found in a recent publication.[27] All measurements were performed in the same in situ spectroscopic cell, thus making the obtained experimental data fully complementary. In Figure 1, scanning electron microscopy (SEM) images of the

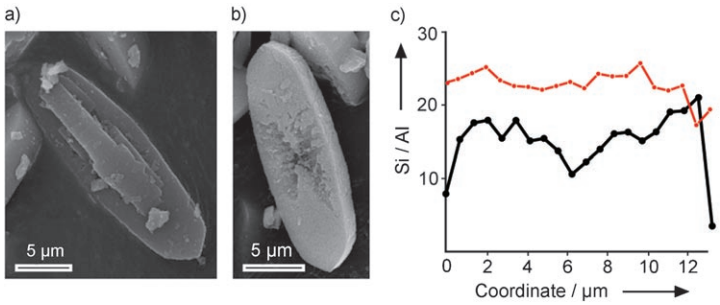

Figure 1. SEM images of the a) microporous and b) mesoporous H-ZSM-5 crystals (size 17×4×4 µm). Scale bar: 5 µm. c) SEM-EDX measurements over the long axis of the microporous (red curve) and mesoporous (black curve) crystals. Experimental error of the Si/Al ratios was estimated to be around 20%.

17×4×4 µm micro- and mesoporous ZSM-5 crystals are presented along with energy-dispersive X-ray (EDX) analysis over the long axis of the crystals. From the SEM images, it can be seen that the morphology of the mesoporous crystals is severely affected by the desilication treatment, leading to a damaged middle part of the crystals. Furthermore, EDX measurements demonstrate that within the experimental accuracy of the method, no aluminum gradient is present in the microporous crystals. In the case of the mesoporous crystals, during the desilication treatment not only silicon is removed from the framework but also, to a lesser extent, aluminum, as reflected by the Si/Al ratio of the filtrate, which was determined to be 1000.[22] In addition, a higher degree of silicon extraction and accompanying mesoporosity formation is expected to occur at the crystal boundaries, that is, the intergrowth regions, leading to an inhomogeneous Si/Al ratio over the long axis of the crystals (Figure 1c). The reported Si/Al ratios are in good agreement with earlier values determined by inductively coupled plasma atomic-emission spectrometry (30 and 24 for microporous and mesoporous crystals, respectively).[24]

Reconstruction of the intergrowth structure of the ZSM-5 crystals by in situ confocal fluorescence microscopy: Zeolitic materials, such as SAPO-5, SAPO-34, and ZSM-5, are not single-crystalline and comprise distinct subunits, evidencing a complex intergrowth structure.[25,28] As the pore geometries in the different building blocks within each of these structures are not always identical, this phenomenon has a large effect on the accessibility of the pores in different regions of the crystals, which may, therefore, significantly

affect the catalytic activity. To investigate the intergrowth structure of the micro- and mesoporous ZSM-5 crystals under study, the as-synthesized crystals were calcined at 773 K for 1 h, cooled to room temperature, and confocal fluorescence images were taken. This allows reconstruction of a three-dimensional spatial distribution of the fluorescent species within the specimen. On heating, the template decomposes accompanied by the formation of light-absorbing and -emitting species. As the accessibility of the porous network in the subunits varies,[29,30] following the template removal process in time enables visualization and reconstruction of the individual building blocks. Recently, the intergrowth structure of similar, though larger, ZSM-5 crystals was revealed in this manner.[25]

Figure 2 shows confocal fluorescence images of the microporous ZSM-5 crystals taken after cooling, which reveal the location of the fluorescent species originating from the template removal phenomena. Firstly, from the confocal top-view image (Figure 2a) intense fluorescence is observed in the middle part of the crystal, indicative of more fluorescent species being present in this region than in the outer parts, and suggesting that the different parts are not interconnected. Secondly, examination of the fluorescence patterns in Figure 2b and d leads to more detailed information on the three-dimensional shape of the middle subunit. These side-view images point out that the most intense fluorescence is observed exactly underneath the middle part and is pyramidal in shape. Furthermore, as in the top view, the fluorescence is more intense in this pyramidal part than in the other parts. The fluorescence pattern in Figure 2c, caused by light-emitting species trapped between the individual subunits, further strengthens the presence of pyramidal boundaries between different subunits. Based on these findings, a three-dimensional model of the crystals is presented in Figure 3, showing the individual building blocks of the boat-shaped crystals; they comprise three building blocks, of which the two smaller units, referred to as the upper and lower lids, have pyramidal boundaries with the largest unit. The arrows indicate the fluorescence images that contributed to the reconstruction of that part of the crystal.

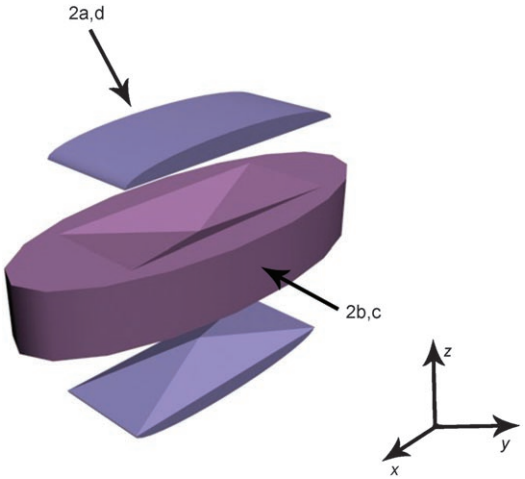

Figure 3. Proposed intergrowth structure and building blocks of the twinned ZSM-5 zeolite crystals under study, based on the images from Figure 2. The *x*, *y*, and *z* directions are indicated.

Revealing the catalytic activity trends in micro- and mesoporous ZSM-5 crystals: To investigate the effect of mesoporosity on the catalytic activity, the oligomerization of different styrene compounds has been used as a probe reaction.[26,27] In Figure 4, microphotographs of micro- and mesoporous ZSM-5 crystals are presented along with their optical absorption spectra, after addition of 4-methoxy- or 4-chlorostyrene from the liquid phase and heat treatment at 373 K. Inspection of the microphotographs clearly shows a difference in coloration, that is, microporous crystals are most colored in the upper lid, whereas the mesoporous crystals predominantly color at the outer parts of the crystal. These distinct coloration patterns can be accounted for by the desilication treatment. Besides mesoporosity formation, desilication also induces a (partial) removal of the upper lid due to the localized attack of the base. These phenomena are likely to be responsible for

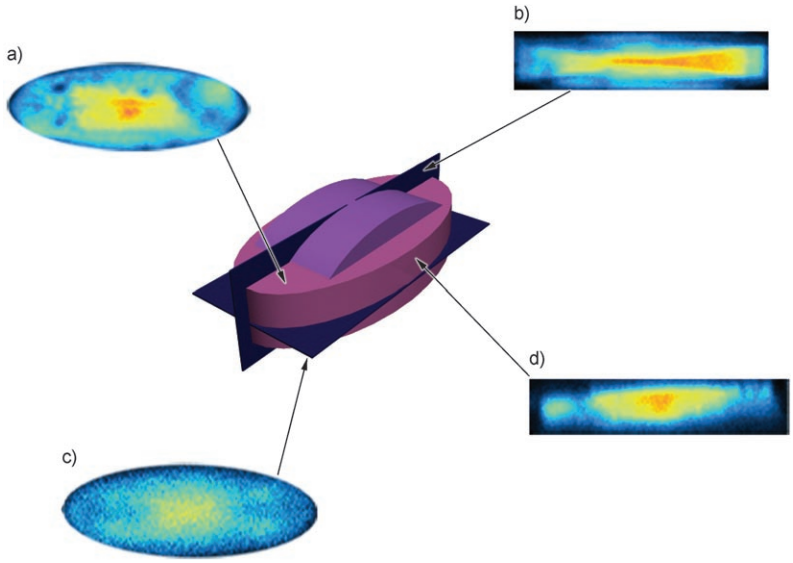

Figure 2. Confocal fluorescence microphotographs of the microporous ZSM-5 crystals measured after the template removal process at 773 K (excitation at 561 nm, detection at 575–635 nm; false colors represent fluorescence intensity). a,b) Top and side views; c,d) horizontal and vertical middle cross sections, respectively.

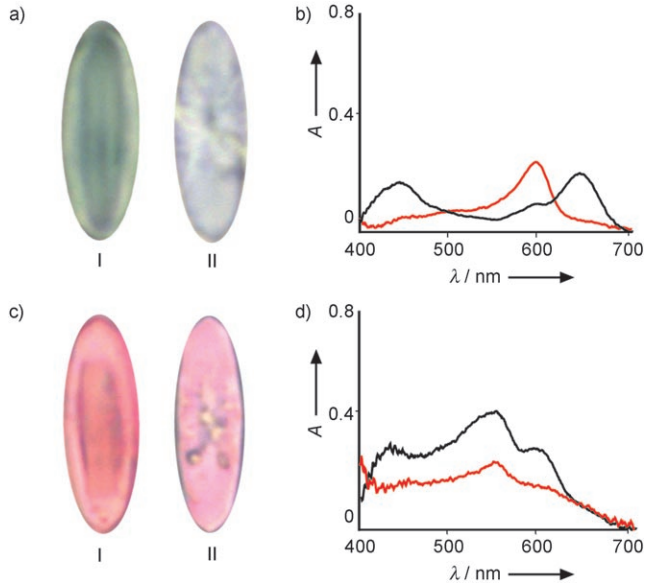

Figure 4. a) Microphotographs of the micro- (I) and mesoporous (II) crystals after oligomerization with 4-methoxystyrene and b) the corresponding optical absorption spectra for the microporous (black curve) and mesoporous (red curve) ZSM-5 crystals. c,d) Same as (a,b) but after oligomerization with 4-chlorostyrene. Measurements were performed ≈5 min after exposure at 373 K.

the more evenly distributed coloration over the crystals. Most probably, the upper lid of the microporous crystals limits to some extent the diffusion of styrene monomers inside the crystal, leading to strong coloration of merely the upper lid in the microporous crystals and a more evenly distributed coloration in the mesoporous ones. Furthermore, as a higher degree of silicon extraction occurs in the intergrowth regions, the accessibility to the various subunits will be improved.

In the optical absorption spectra of the microporous crystals, the presence of two absorption bands can be observed at 595 and 650 nm for 4-methoxystyrene and at 560 and 600 nm for 4-chlorostyrene. The high-energy absorption band has been ascribed to the presence of dimeric carbocation intermediates, whereas the other band originates from trimeric carbocations or higher oligomers. More detailed information on the oligomerization reaction can be found elsewhere.[26,27,31,32] Comparison of the absorption spectra for micro- and mesoporous ZSM-5 crystals shows that, upon desilication, the band intensities associated with dimeric and trimeric carbocation species are changing. More specifically, the longer-wavelength absorption band, present in the microporous crystals, vanishes completely when the oligomerization is carried out over the mesoporous zeolite, showing that in the latter case the formation of trimeric or higher carbocations is limited. This observation can be explained by the following. When purely micropores are present, after dimerization proceeding on Brønsted acid sites, the product molecules may encounter other acid sites, leading to trimeric or higher oligomers. On the contrary, when mesopores are also present, the overall length of the micropores is effectively shortened (by two orders of magnitude).[24] As a consequence, the chance of successive reactions over other Brønsted acid sites leading to the formation of higher oligomers is decreased.

To further examine the reactivity differences between the micro- and mesoporous crystals, the same set of experiments as described above was carried out and confocal microscopic images were acquired. From examination of the fluorescence snapshots of the micro- and mesoporous ZSM-5 crystals (Figure 5), measured inside the spectroscopic cell after

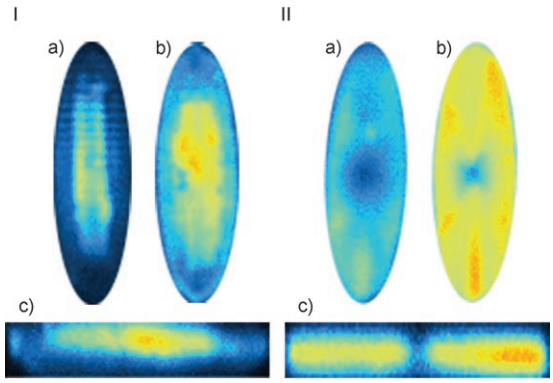

Figure 5. Confocal fluorescence images measured in the in situ spectroscopic cell after oligomerization of 4-methoxystyrene at 373 K on microporous (I) and mesoporous (II) crystals (excitation at 561 nm, detection at 580–640 nm, false color). Indices a)–c) correspond to the upper horizontal plane, middle horizontal plane parallel to the upper plane, and vertical intermediate plane, respectively. Measurements were performed ≈5 min after exposure to the styrene compound.

addition of 4-methoxystyrene, it is clear that the fluorescence pattern is in line with the degree of coloration measured with the optical microscope: more intense fluorescence from the upper lid in the case of the microporous crystals, and a more evenly distributed fluorescence pattern for the mesoporous crystals. Furthermore, fluorescence images of the vertical middle plane in the crystal (Figure 5c) show that the formation of carbocation intermediates after oligomerization with 4-methoxystyrene is not only limited to the upper plane. Finally, comparison of the micro- and mesoporous crystals shows that the fluorescence signal is most intense in the latter case, which can be rationalized by using the optical absorption spectra, that is, the optical absorption in the excitation wavelength (561 nm) directly corresponds to the fluorescence intensity of the crystals. More specifically, in the case of 4-methoxystyrene the absorption in this region is more intense for the mesoporous zeolite, thus leading to a much stronger fluorescence intensity compared to the purely microporous zeolite.

In recent publications,[26,27] we have demonstrated that the oligomerization of various substituted styrene derivatives in H-ZSM-5 crystals leads to distinct catalytic activities, that is, less electron-withdrawing substituents induce an enhancement of the reactivity, whereas bulky styrene compounds do not react due to severe diffusion limitations. As a result of

this, with differently substituted styrene derivatives in hand, the oligomerization reaction provides a good means of studying the effect of mesoporosity on the shape selectivity and catalytic activity. More specifically, bulky styrene derivatives should show no activity in microporous crystals due to size exclusion, but some degree of activity can be expected in the desilicated ones due to the presence of mesopores. This is a suitable approach to demonstrate reactivity in the mesoporous channels. In that case, mesopores do not merely possess a transport function, but can be directly involved in the catalytic process. To investigate this, different styrene compounds were added to the micro- and mesoporous crystals, and confocal fluorescence images were taken in the course of the oligomerization reaction. Firstly, it appeared that bulky compounds, such as *trans*-β-methyl- and β-methoxystyrene, which are not very reactive in microporous crystals, show no reactivity in the case of mesoporous ZSM-5. These observations are in contrast to the expectation that mesopores would facilitate the reaction of larger reactant molecules, suggesting that the mesopores do not partake in the catalytic reaction but merely act as highways to the active sites. Another plausible explanation for this behavior is that the Brønsted acidity in the crystals after desilication is locally affected, and, therefore, they lack sufficient acid strength.[33] As a result of this decrease in acid strength, the Brønsted acid sites would not be capable of protonating less reactive styrene compounds.

To examine this hypothesis, confocal fluorescence images were taken after oligomerization with different styrene compounds that vary in their reactivity. The results are shown in Figure 6, in which clear differences in the fluorescence patterns can be observed. Comparison of 4-methoxy- and 4-ethoxystyrene shows that the fluorescence in the latter case is less evenly distributed over the crystal. 4-Bromostyrene shows a fluorescence pattern more similar to that of 4-methoxystyrene, whereas the other halogen-substituted styrene compounds are merely fluorescent at the edges of the crystals. Rationalization of these observations was attempted by assuming that a gradient in Brønsted acid strength is present in the crystals due to a distinct Si/Al ratio in different parts of the crystals. Consequently, very reactive styrene compounds, such as 4-methoxy- and 4-bromostyrene,[26,27] will react on both strong and weak Brønsted acid sites, leading to a more evenly distributed fluorescence pattern. Styrene compounds with more electronegative substituents, such as 4-chloro- and 4-fluorostyrene, will only react on very strong Brønsted acid sites. By following this line of reasoning the intermediate fluorescence behavior of 4-ethoxystyrene can be easily interpreted by its intermediate reactivity, as was shown previously.[27] These observations suggest that a gradient in the Brønsted acid strength is present in the ZSM-5 crystals, and that the strongest acidic sites are located at the edges of the crystal and the weaker Brønsted acidity is found in the central parts.

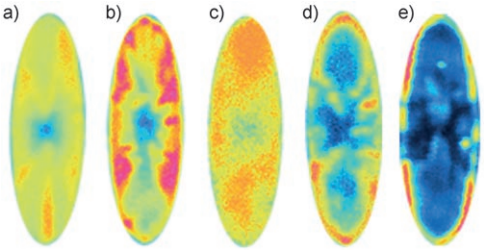

Figure 6. Confocal fluorescence images of the mesoporous crystals measured in the in situ spectroscopic cell after styrene oligomerization with a) 4-methoxy-, b) 4-ethoxy-, c) 4-bromo-, d) 4-chloro-, and e) 4-fluorostyrene (excitation at 561 nm, detection at 580–640 nm, false color). Images of the intermediate horizontal plane parallel to the upper plane are shown. Measurements were performed ≈5 min after exposure.

So far, we have shown that the ZSM-5 crystals are constructed of an upper lid and two other large pyramidal subunits (Figure 3) and that carbocation intermediates are mainly formed within the upper-lid subunit. Upon alkaline treatment, the upper lid is removed and product molecules can more easily diffuse to the interior of the crystal, leading to a more evenly distributed carbocation formation process. The coloration and fluorescence behavior is general for all the crystals studied, with the exception of the mesoporous crystals after oligomerization of 4-methoxystyrene. Strikingly, it was found that most of the mesoporous crystals break apart during oligomerization with 4-methoxystyrene, revealing more detailed information on the crystal morphology. The fragmentation is likely to be attributable to local stresses induced by the exothermal oligomerization reaction. To the best of our knowledge, this is the first time that the fragmentation of zeolite catalyst crystals during reaction has been visualized by using in situ spectroscopic techniques.

Close examination of the confocal fluorescence images of the mesoporous crystals after styrene oligomerization (Figure 5, II b) indicates the presence of more complex crystal morphology than that suggested in Figure 3. More specifically, the fluorescence is not uniform in all parts of the mesoporous crystals, being the most intense in between the subunits. Images of the mesoporous crystals after oligomerization with 4-methoxystyrene clearly show that the crystals are built up of a more complex structure (Figure 7). All

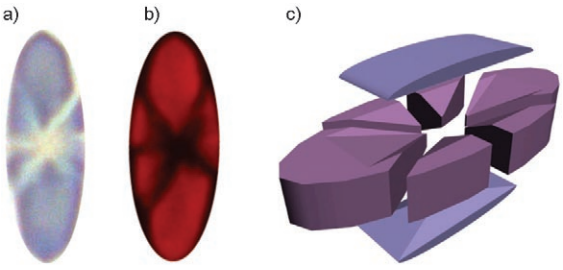

Figure 7. Images of the mesoporous ZSM-5 crystals after oligomerization with 4-methoxystyrene at 373 K measured with a) an optical microscope and b) a fluorescence microscope using light in the region of 510–560 nm from a mercury source. Measurements were performed ≈5 min after exposure. c) A more detailed schematic representation of the ZSM-5 crystal showing its individual building blocks.

these individual units are evenly colored and fluorescent, indicating that before the mesoporous crystals fall apart the styrene monomers oligomerize on the Brønsted acid sites. Furthermore, these cracked crystals are not an exception; about 80% of the crystals are cracked into the same subunits during oligomerization with 4-methoxystyrene. Therefore, we deduced the general schematic representation of the crystals shown in Figure 7. Thus, instead of three building blocks the crystals appear to comprise eight building blocks, which all have pyramidal boundaries with each other. Notably, the architecture of the building blocks closely resembles the silicon concentration profiles determined by SEM-EDX.[14]

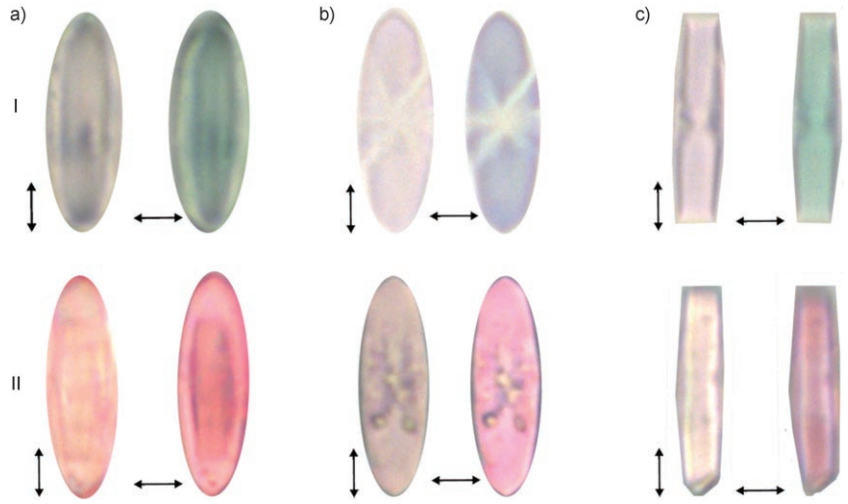

Figure 8. In situ optical microphotographs obtained by using polarized light measured after oligomerization with 4-methoxy- (I) and 4-chlorostyrene (II) at 373 K, for a) microporous and b) mesoporous ZSM-5 crystals; c) side views of microporous crystals. Light polarization is indicated by the arrows.

Elucidating the pore orientation in the different subunits by using polarized-light microscopy: Intergrowth structures, such as those shown in Figure 7, may have a large effect on the accessibility of the micropores in different regions of the crystals and, therefore, affect the catalytic performance.[26,27] Consequently, it is important to gain more insight into the pore orientation within each of the different building blocks. To achieve this, optical microscopy by using polarized light was carried out. As previously shown for large $100\times20\times20$ μm microporous ZSM-5 crystals, the molecular orientation of product molecules can be readily visualized with polarized light.[26,27] When light polarization, that is, the projection of the electrical field vector, is parallel to the dipole moment of a photophysically active molecule, the molecule will absorb light. As the styrene oligomerization for micro- and mesoporous crystals also occurs within the pores of the zeolite, the product molecules are expected to be trapped and aligned within the straight channels of the crystals. This can be confirmed, as a severely bent conformation of the 14 Å-long carbocation intermediates should be imposed in order to become aligned within the zigzag pores. As a consequence, the alignment of the molecules provides information on the direction of the straight pores.

After exposure of the micro- and mesoporous crystals to 4-methoxy- and 4-chlorostyrene, the crystals were measured with the optical microscope by using polarized light. Images of the micro- and mesoporous crystals with 0 and 90° light polarization are presented in Figure 8, for both the top and side views. In the case of the latter, only the microporous crystal images are shown, as the polarization dependence of the side view is identical for the micro- and mesoporous crystals. In the case of the microporous crystals, one can see that when the light polarization coincides with the direction of the short crystal axis ($\theta=90°$), the upper lid of the crystal is intensely colored, but vanishes almost completely when the polarization is directed otherwise ($\theta=0°$). The same polarization dependence is valid for the mesoporous crystals and the crystals viewed from the side.

To further support the coloration behavior upon light polarization, the angular dependence of the absorption band intensity corresponding to the dimeric species (595 and 560 nm, respectively) for 4-methoxy- and 4-chlorostyrene is presented in Figure 9. This angular dependence follows the $\sin^2\theta$ law, in which θ is the angle between the long axis of the crystal and the light polarization vector. From this, it can be clearly seen that the absorption in the upper lid of the microporous and the outer parts of the mesoporous crystals becomes zero when the light polarization is parallel to the crystal's long axis and is maximum when the light polarization is directed perpendicular to this axis. The same holds for the crystals viewed from the side. This polarization behavior unambiguously points out that in the upper lid, the lower subunits (from examination of the mesoporous crystals), and in the side parts of the crystals, the product molecules, are aligned, which is indicative of the orientation of the straight pores. Moreover, the observed alignment of carbocations suggests that the randomly oriented mesopores do not take part in the catalytic reaction.

From the polarization dependence, a schematic representation is deduced (see Figure 10) for the (y,z) and (x,z) planes of the crystals. By using this model, the difference in catalytic/coloration behavior between micro- and mesoporous crystals can be better understood. In the case of microporous crystals, the straight pores of the upper lid can be easily accessed via the zigzag pore openings. The other parts of the upper (x,y) plane, on the contrary, possess fewer

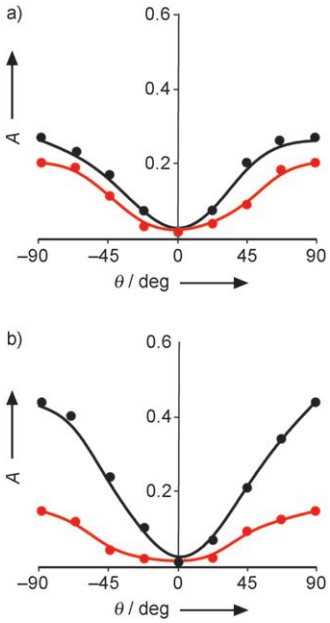

Figure 9. Polarization dependence of the optical absorption after oligomerization with a) 4-methoxy- and b) 4-chlorostyrene at 373 K for the microporous (black curves) and mesoporous (red curves) crystals.

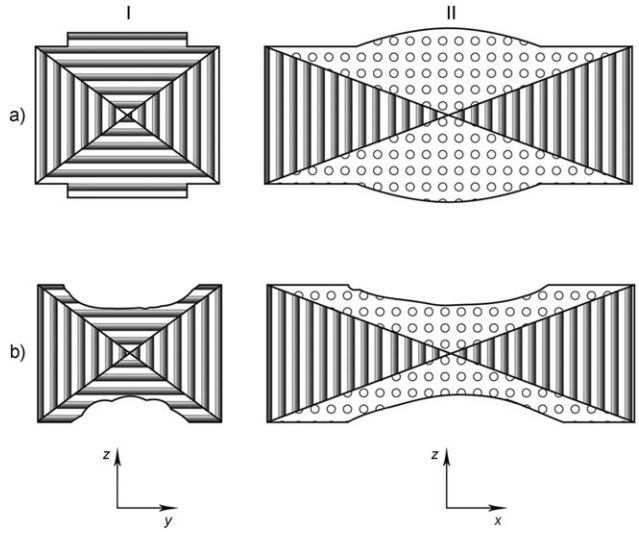

Figure 10. Schematic representation of the straight-pore orientation within a) microporous and b) mesoporous ZSM-5 crystals. Images on the left (I) show the straight-pore orientation in the (y,z) plane, and images on the right (II) in the vertical (x,z) plane. Straight pores are indicated by the horizontal and vertical lines. Circles indicate that the straight pores run in the y direction. The x, y, and z directions are indicated by arrows. Coordinates correspond to those in Figure 3.

zigzag pore openings, thus leading to lower accessibility and, therefore, showing less coloration. As the upper lid is removed during desilication, the outer parts of the crystal become more accessible as reactant molecules can now also enter the straight pores via the middle part of the crystal (Figure 10b).

Conclusions

The combined use of confocal fluorescence and optical absorption microscopy provides valuable insight into the intergrowth structure and catalytic activity trends of ZSM-5 crystals. The combined method has been applied to studying the effect of mesoporosity, introduced into ZSM-5 crystals by using desilication as a postsynthesis treatment. The use of confocal fluorescence microscopy to study the template removal process and the oligomerization with 4-methoxystyrene showed that the micro- and mesoporous ZSM-5 crystals comprise at least eight building blocks, which have pyramidal boundaries with each other. Introduction of mesoporosity[34] enhances the selectivity towards dimeric carbocation intermediates, as the micropore diffusion path length is reduced, thereby suppressing the formation of higher oligomerization products. Furthermore, the diffusion of reactant molecules inside the zeolite crystals is enhanced, leading to a more evenly distributed coloration of the ZSM-5 crystals. The mesopores appear not to participate to a large extent in the catalytic reaction, but serve mainly as highways to the active sites, because bulky styrene compounds are less reactive in the mesoporous crystals than the microporous ones. This conclusion is confirmed by polarization studies of the molecular alignment. Moreover, the oligomerization reaction of different styrene molecules revealed a nonuniform Brønsted acidity over the volume of the mesoporous ZSM-5 crystals, which gradually decreases towards the center of the crystal. Finally, polarized light measurements allowed mapping of the pore orientation in all different subunits of the crystals.

From a more general perspective, this characterization study demonstrates the large possibilities for catalyst scientists, when combining various in situ microspectroscopic methods with suitable active reporter molecules for deducing mechanistic and structural insights down to the molecular level. Provided with the possibility of substantially enlarging the set of suitable reporter molecules, and by increasing the spatial resolution even further, it should become feasible to disentangle diffusion and reactivity patterns within porous catalytic solids in three dimensions at the nanometer scale.[35]

Experimental Section

Materials and experiments: Micro- and mesoporous H-ZSM-5 crystals with a Si/Al ratio of 25 were prepared as documented elsewhere.[24] The Si/Al ratio was determined by SEM-EDX measurements. Styrene derivatives (Acros Organics and Aldrich) were used as received. The microspectroscopic analysis of the H-ZSM-5 crystals was performed in an in situ cell (FTIR 600, Linkam Scientific Instruments) equipped with a temperature controller (Linkam TMS 93). In catalytic experiments, the crystals were submerged in liquid styrene compounds and subsequently heated to the required temperature in the in situ cell.

In situ optical microspectroscopy setup: The setup was based on an Olympus BX41 upright research microscope with a 50× 0.5 NA-high (NA: numerical aperture) working distance microscope objective. A 75-W xenon lamp was used for illumination. The microscope was equipped

with a 50/50 double-viewport tube, which accommodated a CCD video camera (ColorView IIIu, Soft Imaging System GmbH) and an optical fiber mount. A 200-μm-core fiber connected the microscope to a CCD UV/Vis spectrometer (AvaSpec-2048TEC, Avantes). A rotatable polarizer was introduced between the objective and detector to separate the desirable light polarization.

In situ confocal fluorescence microscopy setup: A Nikon Eclipse LV150 upright microscope with a 50× 0.55 NA dry objective was used for fluorescence studies. Fluorescence microphotographs were collected by using 510–560 nm excitation from a mercury source, and confocal images were acquired with a Nikon D-Eclipse C1 head connected to laser light sources (405, 488, and 561 nm). The emission was detected with three photomultiplier tubes in the ranges 425–475, 510–550, and 575–635 nm, respectively, to avoid channel overlap.

Acknowledgements

This work was supported by the Dutch National Science Foundation (NWO-CW VICI grant) and the National Research School Combination-Catalysis (NRSC-C). We thank Professor Dr. J.A. Moulijn for his contributions to this work. M. Versluijs-Helder is acknowledged for performing the SEM-EDX measurements.

[1] A. Corma, *Chem. Rev.* **1995**, *95*, 559–614.
[2] X. Yang, Y. Feng, G. Tian, Y. Du, X. Ge, Y. Di, Y. Zhang, B. Sun, F.-S. Xiao, *Angew. Chem.* **2005**, *117*, 2619–2624; *Angew. Chem. Int. Ed.* **2005**, *44*, 2563–2568.
[3] A. Corma, M. J. Díaz-Cabañas, J. Martínez-Triguero, F. Rey, J. Rius, *Nature* **2002**, *418*, 514–517.
[4] A. Corma, M. J. Díaz-Cabañas, F. Rey, S. Nicolopoulus, K. Boulahya, *Chem. Commun.* **2004**, 1356–1357.
[5] A. Corma, V. Fornes, S. B. Pergher, T. L. M. Maesen, J. G. Buglass, *Nature* **1998**, *396*, 353–356.
[6] L. M. Huang, W. P. Guo, P. Deng, Z. Y. Xue, Q. Z. Li, *J. Phys. Chem. B* **2000**, *104*, 2817–2823.
[7] C. J. H. Jacobsen, C. Madsen, J. Houzvicka, I. Schmidt, A. Carlsson, *J. Am. Chem. Soc.* **2000**, *122*, 7116–7117.
[8] M. Choi, H. S. Cho, R. Srivastava, C. Venkatesan, D. H. Choi, R. Ryoo, *Nat. Mater.* **2006**, *5*, 718–723.
[9] M. Kustova, K. Egeblad, K. Zhu, C. H. Christensen, *Chem. Mater.* **2007**, *19*, 2915–2917.
[10] S. van Donk, A. H. Janssen, J. H. Bitter, K. P. de Jong, *Catal. Rev.* **2003**, *45*, 297–319.
[11] J. Scherzer, *ACS Symp. Ser.* **1984**, *248*, 157.
[12] P. Kortunov, S. Vasenkov, J. Kärger, R. Valiullin, P. Gottschalk, M. Fé Elía, M. Perez, M. Stöcker, B. Drescher, G. McElhiney, C. Berger, R. Gläser, J. Weitkamp, *J. Am. Chem. Soc.* **2005**, *127*, 13055–13059.
[13] A. H. Janssen, A. J. Koster, K. P. de Jong, *Angew. Chem.* **2001**, *113*, 1136–1138; *Angew. Chem. Int. Ed.* **2001**, *40*, 1102–1104.
[14] J. C. Groen, T. Bach, U. Ziese, A. Donk, K. P. de Jong, J. A. Moulijn, J. Pérez-Ramírez, *J. Am. Chem. Soc.* **2005**, *127*, 10792–10793.
[15] J. C. Groen, A. Brückner, E. Berrier, L. Maldonado, J. A. Moulijn, J. Pérez-Ramírez, *J. Catal.* **2006**, *243*, 212–216.
[16] J. C. Groen, L. Maldonado, E. Berrier, A. Brückner, J. A. Moulijn, J. Pérez-Ramírez, *J. Phys. Chem. B* **2006**, *110*, 20369–20378.
[17] J. C. Groen, J. A. Moulijn, J. Pérez-Ramírez, *Microporous Mesoporous Mater.* **2005**, *87*, 153–161.
[18] J. C. Groen, J. A. Moulijn, J. Pérez-Ramírez, *J. Mater. Chem.* **2006**, *16*, 2121–2131.
[19] J. C. Groen, J. A. Moulijn, J. Pérez-Ramírez, *Ind. Eng. Chem. Res.* **2007**, *46*, 4193–4201.
[20] J. C. Groen, L. A. A. Peffer, J. A. Moulijn, J. Pérez-Ramírez, *Stud. Surf. Sci. Catal.* **2005**, *156*, 401–408.
[21] J. C. Groen, L. A. A. Peffer, J. A. Moulijn, J. Pérez-Ramírez, *Chem. Eur. J.* **2005**, *11*, 4983–4994.
[22] J. C. Groen, T. Sano, J. A. Moulijn, J. Pérez-Ramírez, *J. Catal.* **2007**, *251*, 21–27.
[23] D. Farcasiu, R. Leu, A. Corma, *J. Phys. Chem. B* **2002**, *106*, 928–932.
[24] J. C. Groen, W. D. Zhu, S. Brouwer, S. J. Huynink, F. Kapteijn, J. A. Moulijn, J. Pérez-Ramírez, *J. Am. Chem. Soc.* **2007**, *129*, 355–360.
[25] L. Karwacki, E. Stavitski, M. H. F. Kox, J. Kornatowski, B. M. Weckhuysen, *Angew. Chem.* **2007**, *119*, 7366–7369; *Angew. Chem. Int. Ed.* **2007**, *46*, 7228–7231.
[26] M. H. F. Kox, E. Stavitski, B. M. Weckhuysen, *Angew. Chem.* **2007**, *119*, 3726–3729; *Angew. Chem. Int. Ed.* **2007**, *46*, 3652–3655.
[27] E. Stavitski, M. H. F. Kox, B. M. Weckhuysen, *Chem. Eur. J.* **2007**, *13*, 7057–7065.
[28] E. R. Geus, J. C. Jansen, H. van Bekkum, *Zeolites* **1994**, *14*, 82–88.
[29] E. Lehmann, C. Chmelik, H. Scheidt, S. Vasenkov, B. Staudte, J. Kärger, F. Kremer, G. Zadrozna, J. Kornatowski, *J. Am. Chem. Soc.* **2002**, *124*, 8690–8692.
[30] M. Milanesio, G. Artioli, A. F. Gualtieri, L. Palin, C. Lamberti, *J. Am. Chem. Soc.* **2003**, *125*, 14549–14558.
[31] F. L. Cozens, R. Bogdanova, M. Regimbald, H. Garcia, V. Marti, J. C. Scaiano, *J. Phys. Chem. B* **1997**, *101*, 6921–6928.
[32] S. S. Pollack, R. F. Sprecher, E. A. Frommell, *J. Mol. Catal.* **1991**, *66*, 195–203.
[33] Note that IR studies in the OH stretching region have confirmed the apparent preservation of the Brønsted acidity upon desilication (see ref. [21]).
[34] Based on the obtained microspectroscopic results, we cannot rule out the introduction of macropores along with mesopore formation. However, a similar impact on the catalytic behavior is expected.
[35] M. B. J. Roeffaers, G. De Cremer, H. Uji-i, B. Muls, B. F. Sels, P. A. Jacobs, F. C. De Schryver, D. E. De Vos, J. Hofkens, *Proc. Natl. Acad. Sci. USA* **2007**, *104*, 12603–12609.

Received: October 9, 2007
Published online: January 22, 2008

